Analyst

Accepted Manuscript

ROYAL SOCIETY OF CHEMISTRY

www.rsc.org/analyst

Differential Pulse Voltammetry Detection of Dopamine and Ascorbic Acid by Permselective Silica Mesochannels Vertically Attached to the Electrode Surface

Wanzhen Li, Longhua Ding, Qiaohong Wang, Bin Su*

Silica mesochannels vertically aligned on the electrode surface has been employed for permselective detection of dopamine and ascorbic acid.

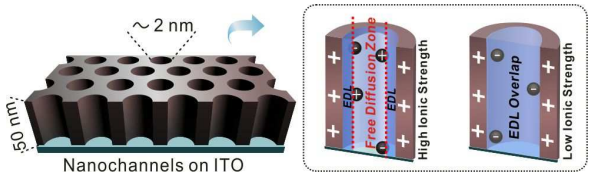

Analyst

RSCPublishing

ARTICLE

Differential Pulse Voltammetry Detection of Dopamine and Ascorbic Acid by Permselective Silica Mesochannels Vertically Attached to the Electrode Surface

Cite this: DOI: 10.1039/x0xx00000x

Received 00th January 2012,
Accepted 00th January 2012

DOI: 10.1039/x0xx00000x

www.rsc.org/

Wanzhen Li, Longhua Ding, Qiaohong Wang, Bin Su*

Thin film consisting of highly ordered and vertically oriented silica mesochannels (SMCs) was prepared on the indium tin oxide (ITO) coated glass electrode surface by chronopotentiometry. The mesochannel has a uniform pore size of 2 ~ 3 nm in diameter and a positively charged surface due to grafted ammonium groups. The electrostatic and steric effects resulted from control of the surface charge and the ionic buffer concentration make the SMCs permselective, favoring the mass transport of oppositely charged species and repelling that of similarly charged ones. By using differential plus voltammetry (DPV), the SMCs with this charge selectivity can be employed for permselective detection of ascorbic acid (AA) and dopamine (DA) that are oppositely charged compounds. The obtained linear detection range was 49 ~ 2651 μM for AA and 20 ~ 226 μM for DA, respectively. AA and DA in real samples were also determined by the SMC film modified electrode.

Introduction

Ascorbic acid (AA) is a commonly used antioxidant and plays an important role in many biological processes. Dopamine (DA) is also a crucial neurotransmitter and its anomalous level represents an indication of neurodegenerative disorders. The determination of both molecules is thus of great importance in the fields of clinical diagnosis and biomedical chemistry.[1-5] However, the electrochemical oxidation peak potentials of AA and DA are close to each other, leading to the significant overlap of respective voltammetric current responses.[6-9] To overcome this problem, abundant researches have been carried out by modifying the electrode surface with different materials, such as polymers,[10-13] metal nanoparticles,[14-20] carbon nanomaterials[21-27] and other composites.[28, 29] The interaction between the target and these materials mainly relies on the electrocatalytic activity of the latter.

Understanding and control of transport processes at the nanoscale enables the construction of novel devices for molecular separation and chemical analysis,[30, 31] because of the unique characteristics conveyed by nanostructures compared with their larger counterparts, such as the high surface-to-volume ratio and the confinement effect. Not only can the mass transport be dramatically accelerated to enhance the signal-to-noise ratio, but also the molecular characteristics such as size, charge and shape can be sensed.[32-36] In addition, new physical phenomena may come to play at the nanoscale, such as the gated and selective transport phenomenon in nanopores/nanochannels of a size comparable to the Debye length in ionic solutions.[37-40] Herein, we report an alternative approach for the quantitative measurements of AA and DA based on the charge permselectivity of silica nanoporous film (50 nm in thickness; 2 ~ 3 nm in pore diameter) modified electrode, given that AA and DA are oppositely charged species existing in the biological environment.

In this work, thin film consisting of silica mesochannels (SMCs) was prepared on the indium tin oxide (ITO) glass as previously reported.[41] The SMCs are highly ordered and vertically attached to the ITO surface, as shown in **Scheme 1**. A key advantage of such 2-dimensional perpendicularly aligned nanochannel structure, in comparison with 3-dimensional structures, lies in that the mass transport of molecules from solution to the underlyinge electrode surface is unobstructed and even enhanced.[42] In addition, due to the ultrasmall channel size (2 ~ 3 nm in diameter) and the electrostatic effect exerted by the channel wall surface, SMCs are permselective to charged molecules. Although such a permselectivity has been observed previously, e.g., under pH control,[43, 44] their electroanalytical applications remain rather unexplored.[45] As we shall show in this work, SMCs with wall surface modified by ammonium groups (namely with a positively charged surface) can be employed for permselective detection of AA and DA. AA (pK_{a1} = 4.04, pK_{a2} = 11.7) and DA (pK_{a1} = 8.9, pK_{a2} = 10.6) are charged species and carry opposite charges in the appropriate

buffer solution. Based on the permselectivity of SMCs regulated by the buffer ionic strength, a wide linear detection range of 49 ~ 2651 μM was obtained for AA and that of 20 ~ 226 μM for DA. Furthermore, AA and DA in human serum were also determined by the SMC film modified electrode.

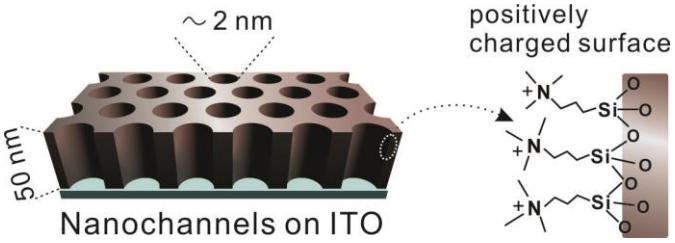

Scheme 1. Illustration of the solid-state SMCs supported on the ITO glass and the positively charged surface due to tethered ammonium groups.

Experimental

Chemicals and reagents

All chemicals and reagents were analytical grade or higher and used as received without further purification. Cetyltrimethylammonium bromide (CTAB, ≥98%), tetraethoxysilane (TEOS, ≥99.0%) and hexaammineruthenium (III) chloride ($Ru(NH_3)_6Cl_3$, 98%) were purchased from Aldrich. *N*-trimethoxysilylpropyl-*N*,*N*,*N*-trimethylammonium chloride (TMAC, 50% in methanol) was received from TCI. Alcohol, sodium nitrate ($NaNO_3$), hydrochloric acid (HCl) and dichloromethane (CH_2Cl_2) were bought from SCRC. AA, DA, potassium hexacyanoferrate (III) ($K_3Fe(CN)_6$), acetic acid (HAc) and sodium acetate (NaAc) were ordered from Aladdin. All aqueous solutions were prepared with high purity water (18 MΩ·cm). Human blood serum was obtained from the Zhejiang University Hospital.

Preparation details of SMCs

SMCs were fabricated by the electro-assisted self-assembly method on ITO plates (surface resistivity ≤ 15 Ω) as reported previously.[41] Typically, a mixture of 20 mL of ethanol and 20 mL of water containing 0.1 M $NaNO_3$ with pH adjusted by HCl to 2.6 was first prepared, to which 13.6 mmol TEOS and 4.35 mmol CTAB were then added under stirring. This obtained precursor sol was further aged for 2.5 h. Then three electrodes (ITO, stainless steel foil and Ag/AgCl/KCl as the working, counter and reference electrodes, respectively) were immersed into the sol. A constant cathodic current density of 0.5 mA cm^{-2} was applied for a certain time to deposit the SMC film on the ITO surface. For the SMC film utilized in this work, the deposition time was 10 s. Subsequently, the ITO electrode was quickly removed from the sol and rinsed with water. After drying under an argon stream and further aging at 130 °C overnight, the template surfactants were extracted from SMCs by immersing the ITO electrodes in 0.1 M HCl/ethanol solution under moderate stirring for 5 min.

Channel surface modification with TMAC

The channel surface modification of SMC film was based on silane coupling reaction.[43] Firstly, the SMCs-coated ITO slide was dried at 100°C for at least 2 h, then treated by 1% (v/v) solution of TMAC in dry dichloromethane for 4 h at room temperature in a Schlek flask under stirring. Finally, the slide was washed in dichloromethane and ethanol sequentially under vigorous stirring, and eventually dried at 80°C for 2 h. It should be noted that the present post-modification method can guarantee a monolayer grafting but not a uniform distribution of the grafted ammonium groups. More groups maybe grafted at the mesopore entrance and less inside the channels.

Instrumentation and measurements

All electrochemical measurements were carried out at room temperature on a CHI 440D (Chenhua, Shanghai) workstation or on an Autolab potentiostat/galvanostat (Eco Chemie, Switzerland). A silver/silver chloride/sat. KCl electrode (Ag/AgCl/sat. KCl) was used as the reference electrode. A stainless steel foil and a platinum wire were used as the counter electrodes for electro-deposition of SMCs and normal electrochemical measurements, respectively. Real sample analysis was performed directly for human blood serum without pretreatment. The recovery value was estimated on the basis of three determinations.

Transmission electron microscopy (TEM) measurement was performed on a HT7700 microscope (HITACHI, Japan) at an acceleration voltage of 120 kV. The samples were prepared by mechanically removing (scraping) some pieces of the SMC film from the ITO surface, which were dispersed in ethanol and then dropped onto the carbon film coated Cu grid. Scanning electron microscopy (SEM) measurement was carried out on a SU-70 (HITACHI, Japan) field emission scanning electronic microscope operating at an accelerating voltage of 3 kV. Quantitative element analysis was done on the basis of x-ray photoelectron spectroscopy (XPS) measurement on the VG ESCALAB MARK II spectrometer (CAE mode, 50 eV, anodes of Mg Kα with radiation at 1253.6 eV).

Results and discussion

SMC films were prepared on the surface of ITO glasses by the electro-assisted self-assembly method as reported previously.[41, 46-48] The preparation is facile and can be finished in seconds. As confirmed by the transmission electron microscopy (TEM) images, electro-deposition of SMCs was successful with highly ordered close-packed nanopores (see top view in **Figure 1a**) and regularly oriented mesochannels (see cross-sectional view in **Figure 1b**). In the high magnification TEM images, mesochannels can be clearly identified with the pore size of 2 ~ 3 nm and a uniform pore density of about 81,000 μm^{-2}. The SMC film is highly organized, mechanically stable, and more importantly it is crack free in terms of electrochemistry data (see **Figure S1**). In addition, the thickness of SMC film can be easily controlled by adjusting the electro-deposition time (see **Figures S2**).The SMC surface has an isoelectric point (IEP) of about 2 ~ 3 and thereby bears negative charges at pH above

IEP.[42] After chemical modification by TMAC (see **Figure S3**), the surface charge was converted from negative to positive (see **Scheme 1**), and meanwhile the channel size decreased by 0.5 nm in diameter.[43, 44, 49] To discriminate, the SMCs after TMAC modification is designated as TMAC-SMCs.

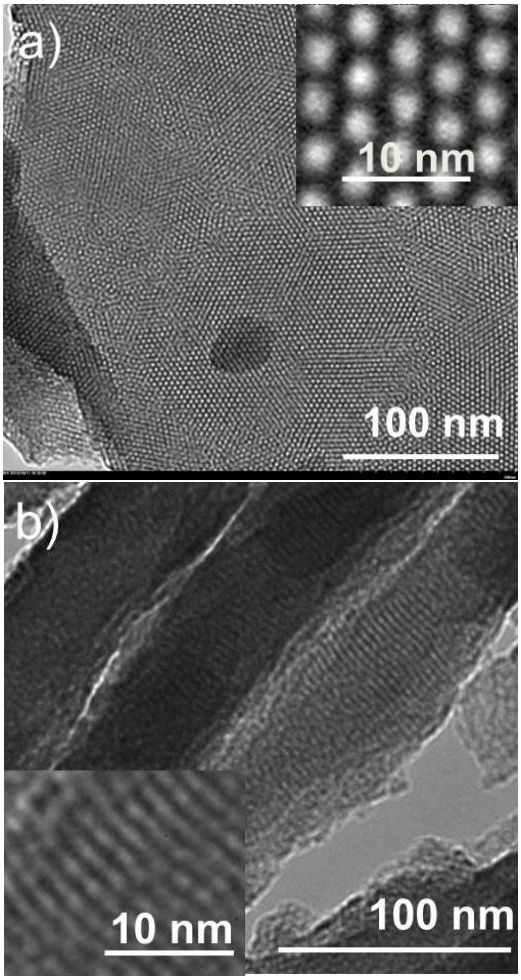

Figure 1. The top (a) and cross-sectional view (b) of TEM images of the SMCs peeled off from ITO surface. The insets correspond to the magnified images showing the nanopores (inset of a) and mesochannels (inset of b).

Electrochemical experiments were performed to examine the surface charge and size of mesochannels. Two eletroactive species bearing opposite charges, $Fe(CN)_6^{3-}$ and $Ru(NH_3)_6^{3+}$, but having almost the same size, were used for this purpose. A comparison between the black and red lines in **Figure 2** suggests that the mass transport of both species from the bulk solution to the underlying electrode through the vertically aligned SMCs was effective. The cyclic voltammogram (CV) of $Ru(NH_3)_6^{3+}$ at the SMC film was very similar to that at a bare ITO, whereas the CV of $Fe(CN)_6^{3-}$ was suppressed significantly. This difference reflects the electrostatic shielding effect of SMCs, favoring the transport of oppositely charged counterions and repelling that of co-ions. However, this situation was completely reversed at the TMAC-SMC film. As shown by the blue curves, the current response of $Fe(CN)_6^{3-}$ turned comparable with that at a bare ITO, while the current signal of $Ru(NH_3)_6^{3+}$ was completely suppressed. Moreover, the current suppression of $Ru(NH_3)_6^{3+}$ by TMAC-SMCs is much more remarkable than that of $Fe(CN)_6^{3-}$ by SMCs, indicating that the electrostatic shielding is much stronger in a smaller mesochennel.

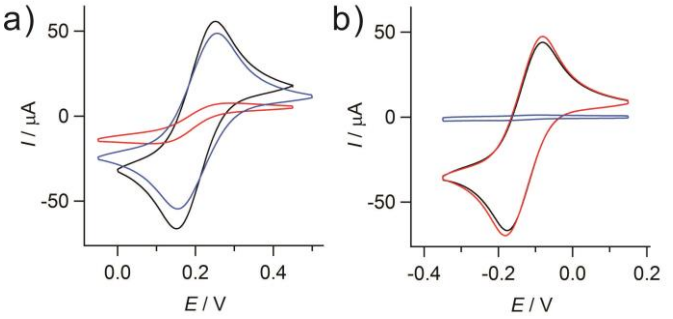

Figure 2. Electrochemical investigation of the permselectivity and permeability of SMCs in 0.1 M acetate buffer (pH 4.5) containing 0.5 mM $Fe(CN)_6^{3-}$ (a) and 0.5 mM $Ru(NH_3)_6^{3+}$ (b): a bare ITO electrode (black), ITO electrodes of the same size covered with the SMCs (red) and TMAC-SMCs (blue). The scan rate was 0.05 V s^{-1} in all cases.

At any charged solid-electrolyte interface, counterions tend to accumulate near the charged surface whereas co-ions are electrostatically repelled. The spatial distribution of ions generates an electric potential profile, which decays to its bulk value over a characteristic length known as the Debye length, λ_D, or called the thickness of electrical double layer (EDL). λ_D is determined by the ionic strength of the electrolyte and can be estimated by the Debye-Hückel approximation:[50]

$$\lambda_D = \sqrt{\frac{\varepsilon_0 \varepsilon k_B T}{2e^2 I_c}} \qquad (1)$$

where I_c is the ionic strength, ε_0 the dielectric permittivity of vacuum, ε the dielectric constant of the solvent, k_B the Boltzman constant, T the absolute temperature and e the electron charge. Using eq. 1, λ_D is calculated to be 0.3 nm, 1.0 nm and 3.1 nm, respectively, for an acetate buffer solution at a concentration of 1.0 M, 0.1 M and 0.01 M.

Therefore, in the case of a cylindrical TMAC-SMC of ~2 nm in diameter, the EDL tends to overlap when the buffer concentration is less than 0.1 M, because the electrostatic surface potential cannot decay completely and remains nonzero even in the centre of the channel (as shown in **Scheme 2a**). In this case, the TMAC-SMCs were forced to be permselective in order to fully compensate the surface charges, thereby attracting the counter-anions and meanwhile repelling the co-cations. This effect accounts for the different cyclic voltammetric behavior of $Fe(CN)_6^{3-}$ and $Ru(NH_3)_6^{3+}$ displayed at the TMAC-SMCs (blue curves in **Figure 2**), because only negatively charged $Fe(CN)_6^{3-}$ was allowed to enter the channels whereas the access of positively charged $Ru(NH_3)_6^{3+}$ was strongly hindered. Indeed, this permselective effect has been investigated in nanofluidic separation and analysis with a

phenomenon of counterion enrichment and co-ion depletion,[51-54] as well as at nanoporous or mesochannel electrodes.[39, 42, 50, 55-58]

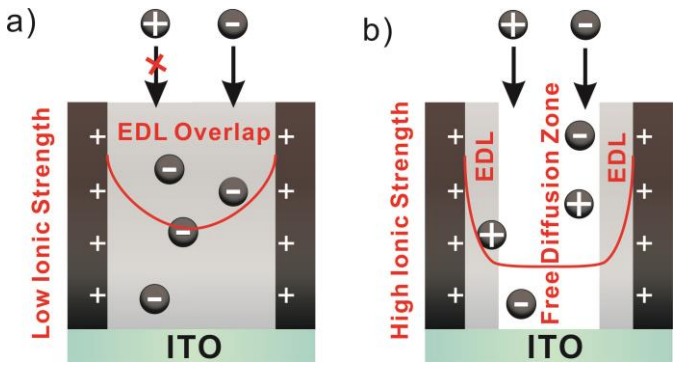

Scheme 2. Schematic comparison of the permselective transport of ions across a positively charged TMAC-SMC modulated by the ionic strength. The gray zone represents the electrical double layer (EDL) and the red curve denotes the imaginary electrostatic potential profile. a) and b) represent the situations under a low and high ionic strength, respectively.

Upon increasing the buffer electrolyte concentration, the EDL thickness decreases and free transport zone in the centre of mesochannel comes to play (see **Scheme 2b**). For example, when the acetate buffer concentration was increased to a value higher than 0.5 M, the TMAC-SMCs became permeable to $Ru(NH_3)_6^{3+}$ and its current response was observed, as shown in **Figure 3a**. It should be noted that the current response of $Fe(CN)_6^{3-}$ remained unaffected by the ionic strength (as seen in **Figure 3b**, a very low buffer concentration produced a high uncompensated solution resistance, thereby leading to a big peak-to-peak separation).

Similar permeselective behaviour was also displayed by the unmodified SMCs bearing negative surface charges, as shown by CVs in **Figure 1** (red curves) and **Figure S4**. However, given that its diameter is larger than TMAC-SMCs by ca. 0.5 nm, an even lower buffer concentration, namely 0.01 M, was required to achieve permselectivity.

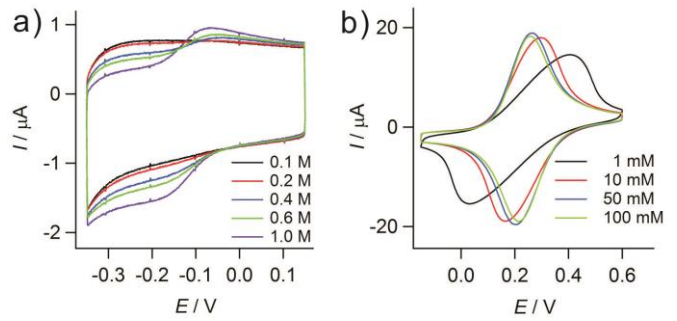

Figure 3. Voltammetric responses of TMA-SMC electrode in aqueous solutions containing 30 μM $Ru(NH_3)_6^{3+}$ (a) and 30 μM $Fe(CN)_6^{3-}$ (b) at various concentrations of acetate buffer. All measurements were done at a scan rate of 0.05 V s^{-1}.

In the following, permselective TMAC-SMCs were applied to distinguish and detect dopamine (DA, pK_{a1} = 8.9, pK_{a2} = 10.6) and ascorbic acid (AA, pK_{a1} = 4.04, pK_{a2} = 11.7). DA and AA usually coexist in physiological samples and their electrochemical responses are always convoluted (as shown in Figure S5). In acetate buffer solutions with a pH of 4.5, DA and AA are positively and negatively charged, respectively. It was found that when the buffer concentration was 0.1 M, the TMAC-SMCs are only permeable to AA (see Figure 4a). By increasing the buffer concentration to 1.0 M, DA can also access the TMAC-SMCs while its electrochemical oxidation takes place at a more positive potential than that of AA by 0.36 V (see Figure 4d). In both cases, we observed that the current responses of DA and AA increased with increasing their respective concentrations, whereas the co-existed AA and DA did not display apparent interference, as shown in **Figure 4b** and 4e. The peak current of AA oxidation was proportional to its concentration in a rather wide range from 49 μM to 2651 μM when 0.1 mM DA was present (**Figure 4c**). The linear regression equation is calibrated as $I_{p,AA}$ (μA) = 2.47 + 0.024C_{AA} (μM) (R^2 = 0.9996) and the detection limits (S/N = 3) is 11 μM. Also, it can be seen from Figure 4f that the peak current of DA oxidation was linear with its concentration in the range from 20 μM to 226 μM when 0.1 mM AA was present and the linear regression equation is expressed as $I_{p,DA}$ (μA) = 1.00 + 0.030C_{DA} (μM) (R^2 = 0.9988) with a detction limit (S/N = 3) of 9 μM.

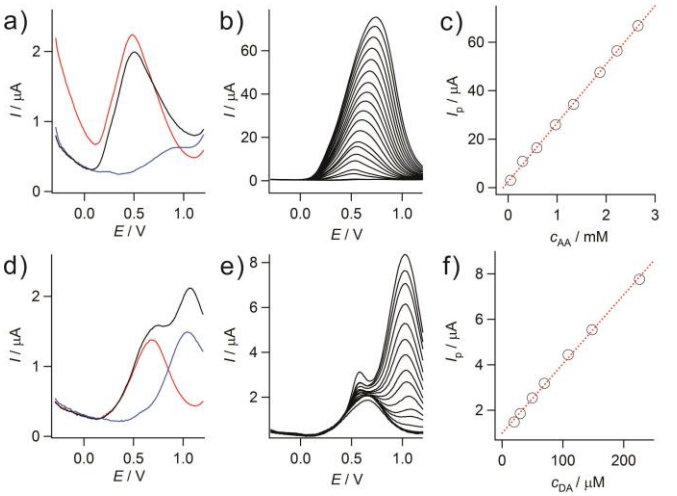

Figure 4. (a, d) DPV responses of TMAC-SMCs in acetate buffer solutions (pH 4.5) of 0.1 M (a) and 1.0 M (d) containing 0.1 mM AA (red), 0.1 mM DA (blue) and both (black), respectively. (b) DPV responses of TMAC-SMCs in 0.1 M acetate buffer (pH 4.5) containing 0.1 mM DA and various concentrations of AA. (e) DPV responses of TMAC-SMCs in 1.0 M acetate buffer (pH 4.5) containing 0.1 mM AA and various concentrations of DA. (c, f) The linear dependence of DPV peak current on the DA, AA concentration, respectively.

To investigate the possibility of the sensor for practical appalications, the TMAC-SMC modified electrode was empolyed for the detection of AA and DA in human blood serum. The human blood serum sample was only diluted 100 times with acetate buffer (pH 4.5) without any other pretreatment. Then various amount of AA or DA stock solution were added into the diluted blood serum solution for electrochemical measurements. The obtained results are

summarized in Table 1. The recoveries indicate that the TMAC-SMC modified electrode can be potentially used for the determination of AA and DA in real samples.

Table 1. Recovery of AA and DA in human blood serum (n = 3).

Samples	Added (mM)	Found (mM)	Recovery (%)
AA	1.00	1.06	105.8
	2.00	1.98	98.9
DA	0.120	0.104	86.7

[a] Average of three determinations.

Conclusions

In summary, we report the selective detection of ascorbic acid and dopamine based on the ionically permselective nature of thin film consisting of silica mesochannels. These silica mesochannels are highly ordered and perpendicularly attached to the electrode surface, and the channel surface is positively charged after modification with ammonium groups. Due to the ultrasmall channel size (diameter of 2 ~ 3 nm) and the surface charge effect, the silica mesochannel film displays clear permselectivity towards ionic species, which can be easily regulated by the buffer electrolyte concentration. Such a property can be employed for selective detection of ascorbic acid and dopamine that carry opposite charges. We believe that this silica mesochannel film consisting of regularly mesochannels, by rationally modulating the surface charge, as well as the steric and hydrophobic effect, will provide a unique platform for designing highly sensitive electrochemical sensors and molecular devices.

Acknowledgements

This work is supported by the national nature science foundation of China (21222504, 21335001), the Program for New Century Excellent Talents in University and the Fundamental Research Funds for the Central Universities (2014XZZX003-04, 2014FZA3006).

Notes and references

Institute of Microanalytical Systems, Department of Chemistry, Zhejiang University, Hangzhou 310058, China Fax: +86 571-88273572; Tel: +86 571-88273496; E-mail: subin@zju.edu.cn

Electronic Supplementary Information (ESI) available: [characterization of mesochannel film by electrochemistry, XPS and SEM]. See DOI: 10.1039/b000000x/

1. M. Zhang, K. Liu, L. Xiang, Y. Lin, L. Su and L. Mao, *Anal. Chem.*, 2007, **79**, 6559-6565.
2. C. Andr é, I. Castanheira, J. M. Cruz, P. Paseiro and A. Sanches-Silva, *Trends Food Sci. Tech.*, 2010, **21**, 229-246.
3. P. Kalimuthu and S. A. John, *Bioelectrochem.*, 2009, **77**, 13-18.
4. J. Ping, J. Wu, Y. Wang and Y. Ying, *Biosens. Bioelectron.*, 2012, **34**, 70-76.
5. D. Sulzer, *Neuron*, 2011, **69**, 628-649.
6. G. Jin, Y. Zhang and W. Cheng, *Sens. Actuators B: Chem.*, 2005, **107**, 528-534.
7. D. Zheng, J. Ye, L. Zhou, Y. Zhang and C. Yu, *J. Electroanal. Chem.*, 2009, **625**, 82-87.
8. C. L. Sun, C. T. Chang, H. H. Lee, J. Zhou, J. Wang, T. K. Sham and W. F. Pong, *ACS Nano*, 2011, **5**, 7788-7795.
9. M. Zhang, K. Gong, H. Zhang and L. Mao, *Biosens. Bioelectron.*, 2005, **20**, 1270-1276.
10. P. Kalimuthu and S. A. John, *Talanta*, 2010, **80**, 1686-1691.
11. H. Yao, Y. Sun, X. Lin, Y. Tang and L. Huang, *Electrochim. Acta*, 2007, **52**, 6165-6171.
12. A. Balamurugan and S. M. Chen, *Anal. Chim. Acta.*, 2007, **596**, 92-98.
13. W. Ren, H. Q. Luo and N. B. Li, *Biosens. Bioelectron.*, 2006, **21**, 1086-1092.
14. D. Sun, Q. Zhao, F. Tan, X. Wang and J. Gao, *Anal. Methods*, 2012, **4**, 3283-3289.
15. Ş. Ulubay and Z. Dursun, *Talanta*, 2010, **80**, 1461-1466.
16. G. Hu, Y. Ma, Y. Guo and S. Shao, *Electrochim. Acta*, 2008, **53**, 6610-6615.
17. S. Thiagarajan and S. M. Chen, *Talanta*, 2007, **74**, 212-222.
18. P. Shakkthivel and S. M. Chen, *Biosens. Bioelectron.*, 2007, **22**, 1680-1687.
19. S. Shahrokhian and H. Zaremehrjardi, *Sens. Actuators B: Chem.*, 2007, **121**, 530-537.
20. C. R. Raj, T. Okajima and T. Ohsaka, *J. of Electroanal. Chem.*, 2003, **543**, 127-133.
21. Y. Yue, G. Hu, M. Zheng, Y. Guo, J. Cao and S. Shao, *Carbon*, 2012, **50**, 107-114.
22. Z. Wang, M. Shoji and H. Ogata, *Analyst*, 2011, **136**, 4903-4905.
23. S. Zhu, H. Li, W. Niu and G. Xu, *Biosens. Bioelectron.*, 2009, **25**, 940-943.
24. R. T. Kachoosangi and R. G. Compton, *Anal. Bioanal. Chem.*, 2007, **387**, 2793-2800.
25. N. Jia, Z. Wang, G. Yang, H. Shen and L. Zhu, *Electrochem. Commun.*, 2007, **9**, 233-238.
26. A. Salimi, H. MamKhezri and R. Hallaj, *Talanta*, 2006, **70**, 823-832.
27. A. Safavi, N. Maleki, O. Moradlou and F. Tajabadi, *Anal. Biochem.*, 2006, **359**, 224-229.
28. Y. Tong, Z. Li, X. Lu, L. Yang, W. Sun, G. Nie, Z. Wang and C. Wang, *Electrochim. Acta*, 2013, **95**, 12-17.
29. H. R. Zare, N. Nasirizadeh and M. Mazloum Ardakani, *J. of Electroanal. Chem.*, 2005, **577**, 25-33.
30. J. J. Kasianowicz, J. W. F. Robertson, E. R. Chan, J. E. Reiner and V. M. Stanford, *Annu. Rev. Anal. chem.*, 2008, **1**, 737-766.
31. P. W. Bohn, *Annu. Rev. Anal. chem.*, 2009, **2**, 279-296.
32. T. Sano, N. Iguchi, K. Iida, T. Sakamoto, M. Baba and H. Kawaura, *Appl. Phys. Lett.*, 2003, **83**, 4438-4440.
33. Y. X. Li and T. Ito, *Anal. Chem.*, 2009, **81**, 851-855.
34. A. L. Garcia, L. K. Ista, D. N. Petsev, M. J. O'Brien, P. Bisong, A. A. Mammoli, S. R. J. Brueck and G. P. Lopez, *Lab Chip*, 2005, **5**, 1271-1276.
35. X. Hou, H. Zhang and L. Jiang, *Angew. Chem. Int. Ed.*, 2012, **51**, 5296-5307.
36. B. N. Miles, A. P. Ivanov, K. A. Wilson, F. Dogan, D. Japrung and J. B. Edel, *Chem. Soc. Rev.*, 2013, **42**, 15-28.

37. G. Wang, B. Zhang, J. R. Wayment, J. M. Harris and H. S. White, *J. Am. Chem. Soc.*, 2006, **128**, 7679-7686.
38. B. Yameen, M. Ali, R. Neumann, W. Ensinger, W. Knoll and O. Azzaroni, *Nano Lett.*, 2009, **9**, 2788-2793.
39. A. Calvo, B. Yameen, F. J. Williams, G. J. Soler-Illia and O. Azzaroni, *J. Am. Chem. Soc.*, 2009, **131**, 10866-10868.
40. C. Amatore, A. I. Oleinick and I. Svir, *Chemphyschem*, 2009, **10**, 211-221.
41. A. Walcarius, E. Sibottier, M. Etienne and J. Ghanbaja, *Nat. Mater.*, 2007, **6**, 602-608.
42. M. Etienne, A. Quach, D. Grosso, L. Nicole, C. Sanchez and A. Walcarius, *Chem. Mater.*, 2007, **19**, 844-856.
43. D. Fattakhova-Rohlfing, M. Wark and J. Rathousky, *Sens. Actuators B: Chem.*, 2007, **126**, 78-81.
44. D. Fattakhova-Rohlfing, M. Wark and J. Rathouský, *Chem. Mater.*, 2007, **19**, 1640-1647.
45. A. Goux, J. Ghanbaja and A. Walcarius, *J. Mater. Sci.*, 2009, **44**, 6601-6607.
46. A. Goux, M. Etienne, E. Aubert, C. Lecomte, J. Ghanbaja and A. Walcarius, *Chem. Mater.*, 2009, **21**, 731-741.
47. Y. Guillemin, M. Etienne, E. Aubert and A. Walcarius, *J. Mater. Chem.*, 2010, **20**, 6799-6807.
48. Y. Guillemin, M. Etienne, E. Sibottier and A. Walcarius, *Chem. Mater.*, 2011, **23**, 5313-5322.
49. D. Fattakhova-Rohlfing, M. Wark and J. Rathousky, in *Studies in Surface Science and Catalysis*, eds. D. Zhao, S. Qiu, Y. Tang and C. Yu, Elsevier, 2007, vol. Volume 165, pp. 573-577.
50. R. Schoch, J. Han and P. Renaud, *Rev. Mod. Phys.*, 2008, **80**, 839-883.
51. H. Daiguji, P. Yang and A. Majumdar, *Nano Lett.*, 2004, **4**, 137-142.
52. Q. Pu, J. Yun, H. Temkin and S. Liu, *Nano Lett.*, 2004, **4**, 1099-1103.
53. R. Karnik, R. Fan, M. Yue, D. Li, P. Yang and A. Majumdar, *Nano Lett.*, 2005, **5**, 943-948.
54. I. Vlassiouk, S. Smirnov and Z. Siwy, *Nano Lett.*, 2008, **8**, 1978-1985.
55. H. Boo, S. Park, B. Ku, Y. Kim, J. H. Park, H. C. Kim and T. D. Chung, *J. Am. Chem. Soc.*, 2004, **126**, 4524-4525.
56. M. Etienne, Y. Guillemin, D. Grosso and A. Walcarius, *Anal. Bioanal. Chem.*, 2013, **405**, 1497-1512.
57. A. Walcarius, *Chem. Soc. Rev.*, 2013, **42**, 4098-4140.
58. A. Brunsen, A. Calvo, F. J. Williams, G. J. Soler-Illia and O. Azzaroni, *Langmuir*, 2011, **27**, 4328-4333.

